eLIFE
elifesciences.org

Figures and figure supplements

Assembly and positioning of actomyosin rings by contractility and planar cell polarity

Ivonne M Sehring, et al.

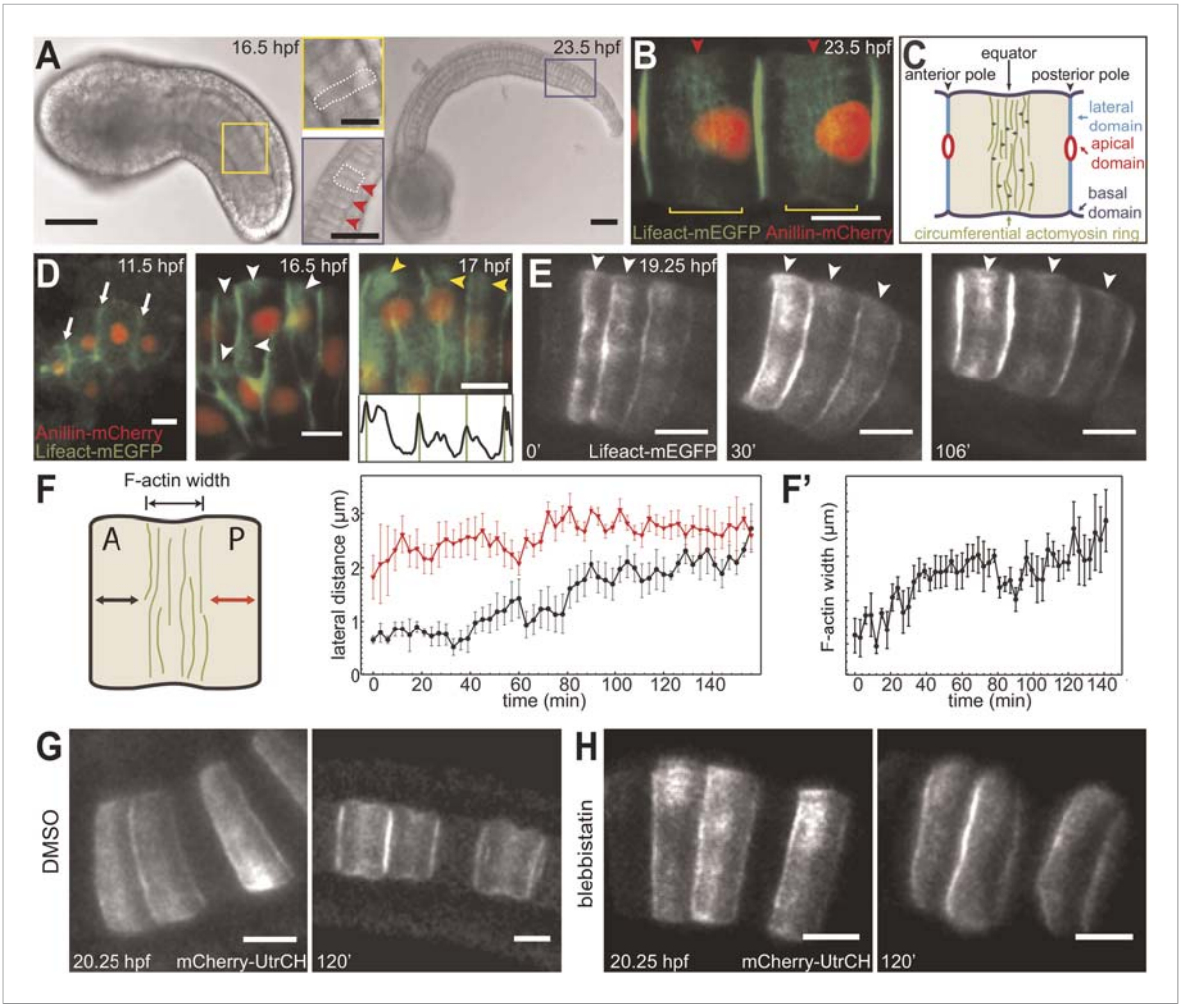

Figure 1. Establishment and relocation of anterior basal cortical actin filaments. (**A**) *Ciona* embryos at 16.5 and 23.5 hr post fertilization (hpf). Following cell intercalation, notochord cells at 16.5 hpf are coin-shaped (one is highlighted in the insert). At 23.5 hpf, cells are cylindrically elongated, and a circumferential constriction is present midway between the two poles (red arrowheads in insert). (**B**) Notochord cells are labeled with Lifeact-mEGFP (green) for actin and Anillin-mCherry (red) for the nucleus. Red arrowheads indicate the equatorial constrictions; yellow brackets outline the circumferential actin rings at the equatorial region. (**C**) A diagram of an elongating notochord cell at the onset of lumen formation with the nomenclature used in this paper. Small dark green arrows indicate the bi-directional cortical flow of actin filaments contributing to the construction of the actin ring. (**D**) Notochord cells labeled with Lifeact-mEGFP (green) for actin and Anillin-mCherry (red) for the nucleus. At the start of intercalation (11.5 hpf), actin is evenly distributed in the cell boundaries (white arrows). During cell intercalation, basal cortical actin patches (white arrowheads) appear adjacent to the anterior lateral domain. The actin patches begin to fuse next to the anterior pole of the cells (yellow arrowheads). The intensity was measured at positions of arrowheads. Vertical green bars indicate lateral domains. (**E**) Notochord cells expressing Lifeact-mEGFP for actin. These images are from ***Video 1***. After cell intercalation, basal cortical actin patches (arrowheads) continue to fuse, forming a circumferential ring next to the anterior lateral domain, which subsequently relocates to the equator, as cells elongate. (**F**) Mean distances between the anterior lateral domain and the cortical actin ring (black), and the posterior lateral domain and the cortical actin ring (red) during cell elongation ($n = 7$; error bars = SEM). (**F'**) Mean ring width over time ($n = 7$; error bars = SEM). (**G**, **H**) Blebbistatin inhibits relocation of anterior basal cortical actin filaments and cell elongation. Notochord cells are labeled with mCherry-UtrCH for actin. Embryos are either treated with DMSO (**G**) or incubated in blebbistatin (**H**) for 120 min. Anterior to the left in all images. Scale bars in **A** represent 50 μm; in inserts, 20 μm; in **B**–**E**, **G**, **H** represent 10 μm.

DOI: 10.7554/eLife.09206.003

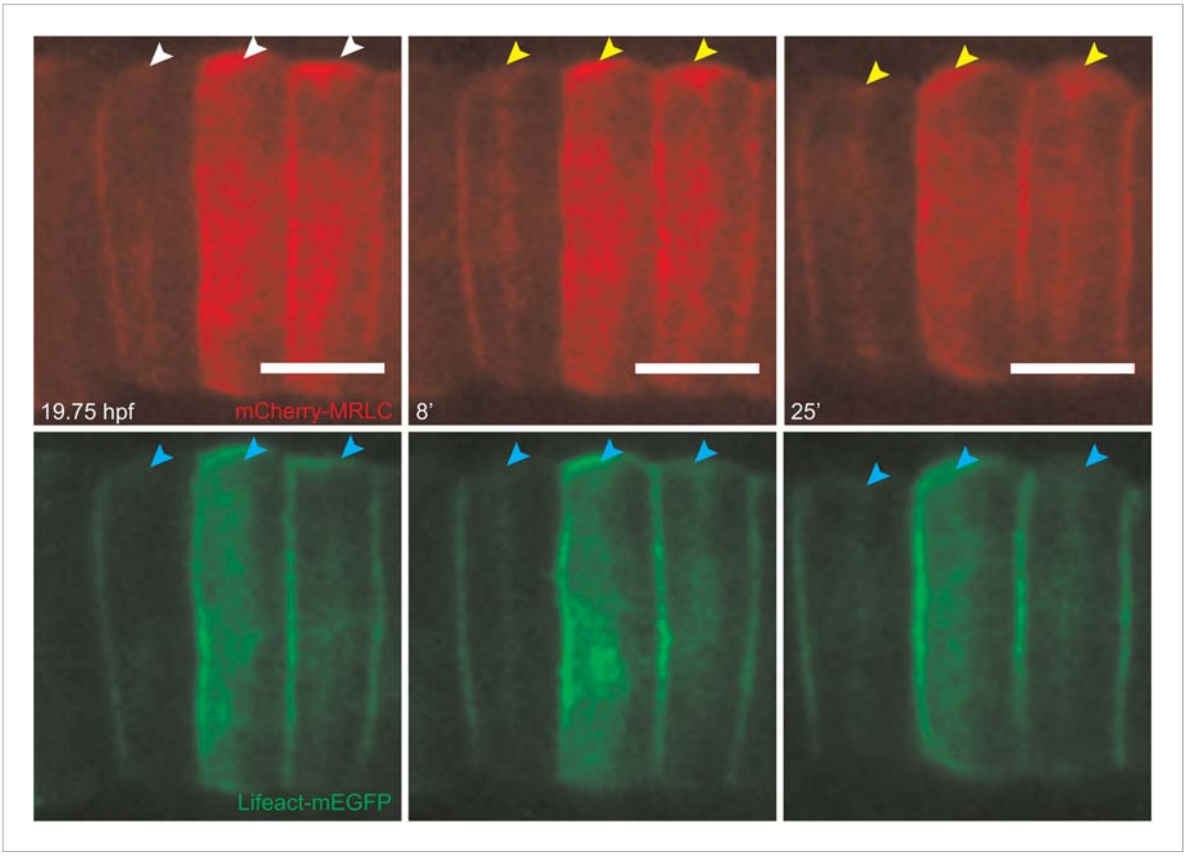

Figure 1—figure supplement 1. Establishment and relocation of anterior basal cortical myosin. Notochord cells expressing mCherry-MRLC (red) and Lifeact-mEGFP for actin (green). In coin-shaped cells, cortical basal myosin is enriched adjacent to the anterior pole (white arrowheads). The myosin ring colocalizes with actin (cyan arrowheads) and relocates towards the equator (yellow arrowheads) during cell elongation. Anterior to the left. Scale bars, 10 μm.

DOI: 10.7554/eLife.09206.004

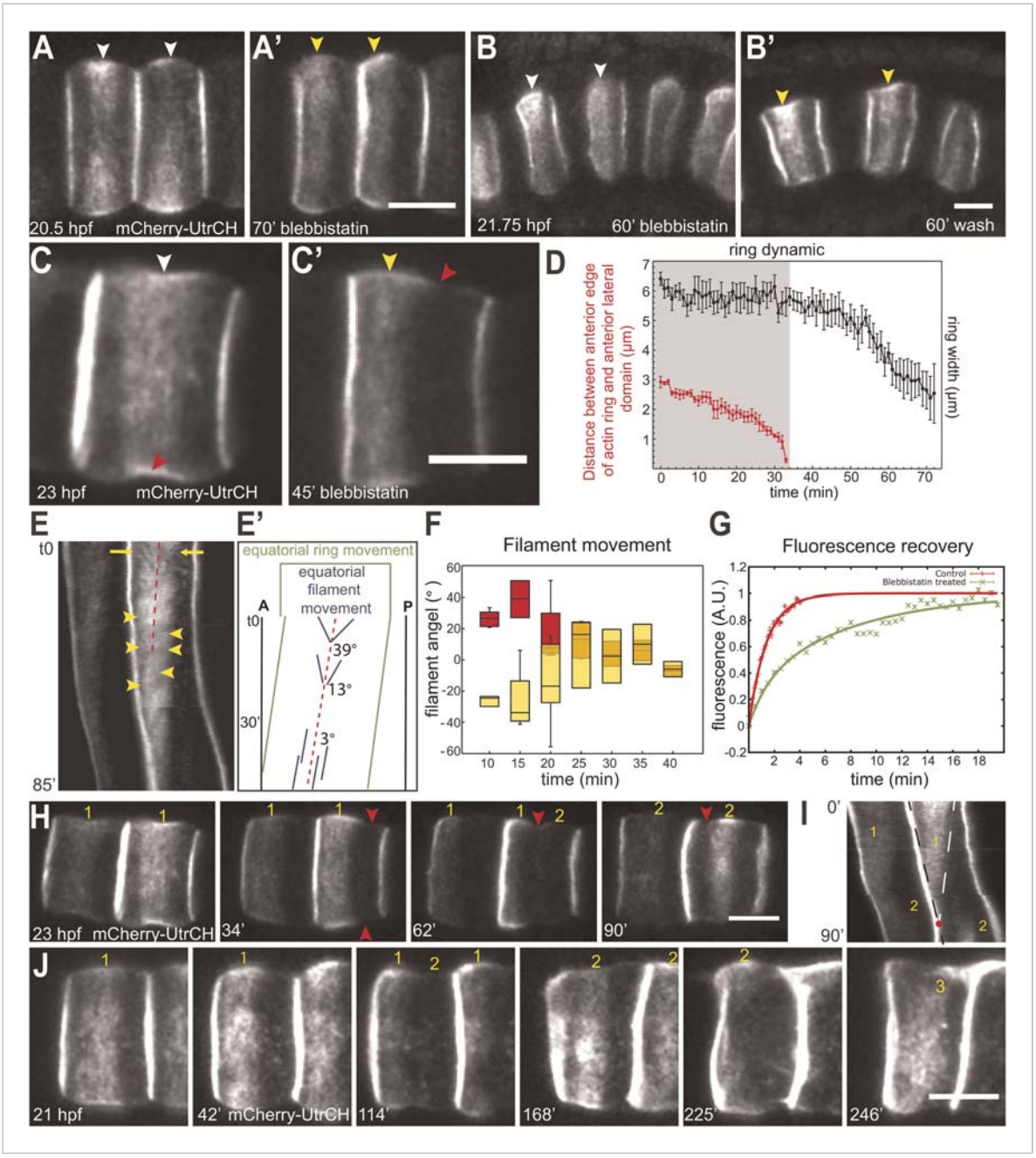

Figure 2. Shifting of equatorial actin filaments upon blebbistatin treatment. Notochord cells are labeled with mCherry-UtrCH or mCherry-hActin for actin. (**A**, **A'**) The equatorial actin ring (white arrowheads) in early elongating cells (**A**, 20.5 hpf) is relocated to the anterior pole (yellow arrowheads) after 70 min blebbistatin treatment (**A'**). (**B**, **B'**) The anterior relocation of the actin ring and inhibition of cell elongation after 60-min blebbistatin treatment (**B**) is reversed by a 60 min wash (**B'**). (**C**) At 23 hpf, the elongated notochord cell has a broad equatorial actin ring (white arrowhead) that is associated with a prominent constriction (red arrowhead). After 45-min blebbistatin treatment, the ring is shifted to the anterior pole (yellow arrowhead), whereas the constriction is not. (**D**) Mean distance between the anterior lateral domain and the middle of the ring (red), and the mean ring width (black) over time. While the ring shifts toward the anterior pole, indicated by the decrease of the anterior basal domain, its width stays relatively constant (shaded in gray). After the ring reaches the anterior lateral domain, the width decreases. $n = 5$; error bars = SEM. (**E**, **E'**) Kymograph of the shifting actin ring based on ***Video 2***. Individual filaments (arrows) from the anterior and posterior edge move towards the center of the ring (the equator, indicated by the dashed line), which itself is shifting anteriorly. After a certain time, the equatorial bound movement of filaments becomes parallel to the movement of the ring (arrowheads). A diagram of the different movements is shown in **E'**. (**F**) Angles of single filament movement at specific times with respect to the center of the ring. Red (positive values), movement from posterior towards the center; yellow (negative values), movement from anterior towards the center. $n = 2–7$; error bars = SEM. (**G**) Fluorescence recovery after photobleaching in cells expressing mCherry-hActin. The entire actin ring region was bleached. Recovery is significantly slower in blebbistatin-treated cells. Control, $n = 4$; blebbistatin, $n = 7$; $p = 0.012$. Solid lines indicate a single exponential fit for the

Figure 2. continued on next page

Figure 2. Continued

control (red curve) with a turnover time of 90 ± 3 s, and a double exponential fit for the blebbistatin treatment (green curve), with a fast fraction with the same turnover as the control, and a slow fraction (f = 70% ± 4%) with a turnover time of 7.8 ± 0.6 min. (**H**) Time-lapse frames of ***Video 3*** showing the anterior movement of the equatorial ring (1), its disappearance, and the emergence of a second ring (2) at the equator. Red arrowheads indicate the circumferential constriction. (**I**) The kymograph illustrates the close succession of the second ring to the first ring. The red dot indicates the time when the first ring disappears at the anterior lateral domain, and the second ring begins to appear. (**J**) Time-lapse frames from ***Video 4*** showing the emergence of a second (2) and third (3) ring with long-term blebbistatin treatment. Anterior to the left in all panels. Scale bars, 10 μm.

DOI: 10.7554/eLife.09206.006

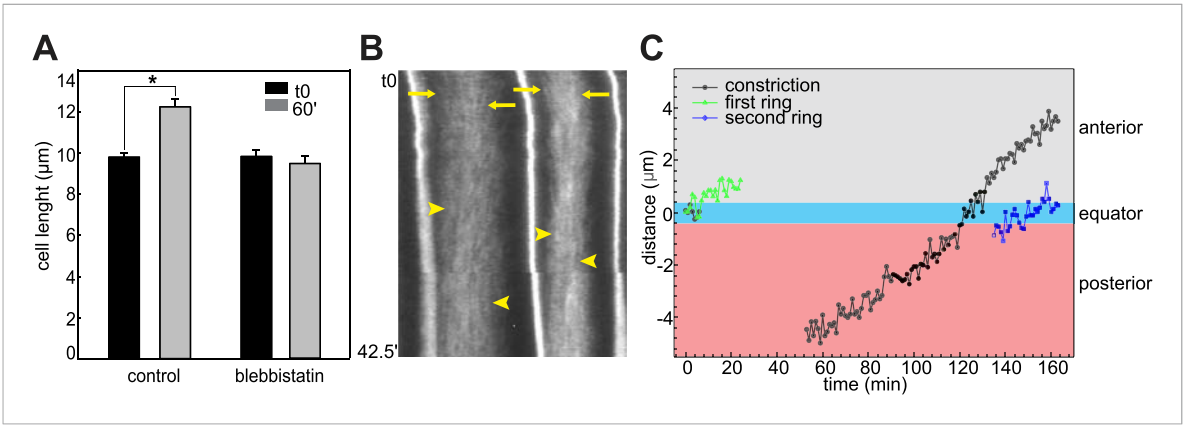

Figure 2—figure supplement 1. Effect of blebbistatin treatment. (**A**) Cell length does not significantly change during ring shifting. *N* = 10; error bars = SEM. (**B**) Kymograph illustrating the directed movement of filaments toward the shifting ring equator (arrows) and the parallel filaments after prolonged incubation (arrowheads). (**C**) Dislodgment of constriction and actin ring from each other and the cell equator. The green graph shows the distance between the middle of the first ring and the cell equator. Measurement stopped when the ring reached the anterior lateral domain. The constriction stayed equatorial (black graph). Between 26 and 39 min, no constriction could be observed. At 40 min, a new constriction emerged posteriorly and shifted anteriorly. The second ring (blue graph) is not associated with the new constriction.

DOI: 10.7554/eLife.09206.007

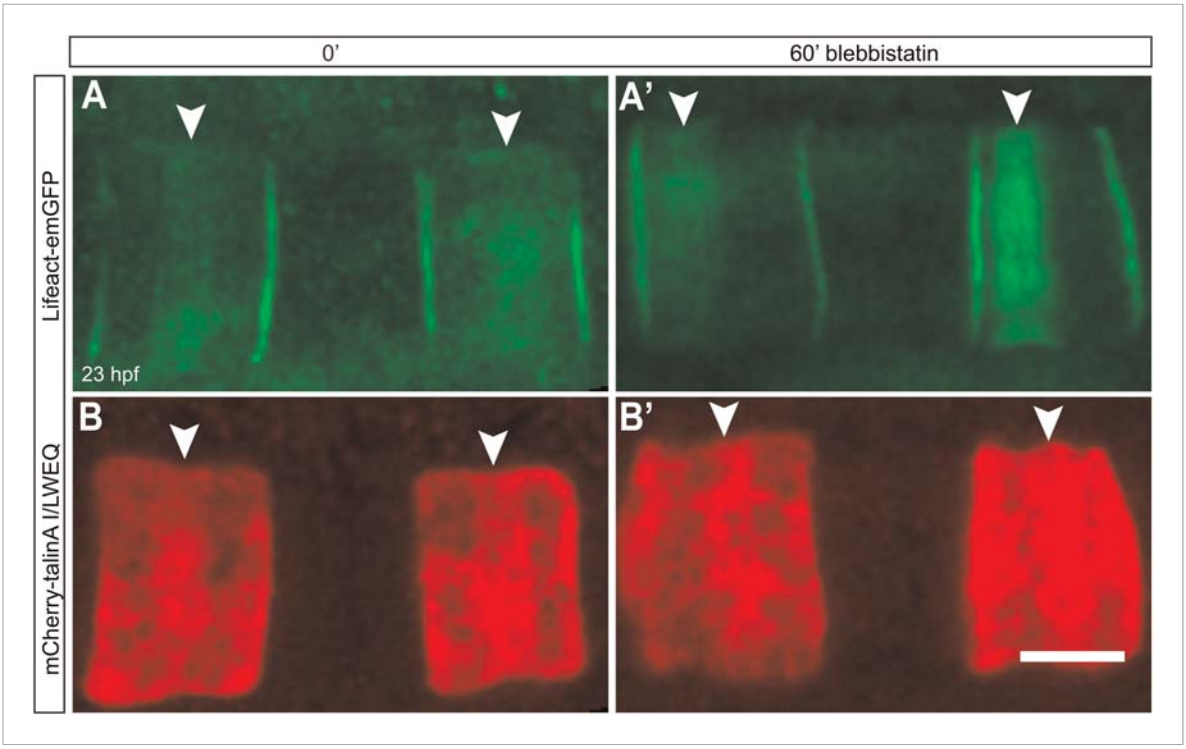

Figure 2—figure supplement 2. Talin localization at the equator is not affected by lower contractility. Notochord cells are labeled simultaneously with Lifeact-mEGFP for actin (**A**, **A'**) and mCherry-talinA I/LWEQ (**B**, **B'**). Both actin and talin are enriched in the equatorial cortex before the blebbistatin treatment (**A**, **B**). After 60-min blebbistatin treatment, actin ring is shifted to the anterior pole (white arrowhead in **A'**), whereas talin remains at the equator (white arrowheads in **B'**). Anterior to the left in all panels. Scale bars, 10 μm.

DOI: 10.7554/eLife.09206.008

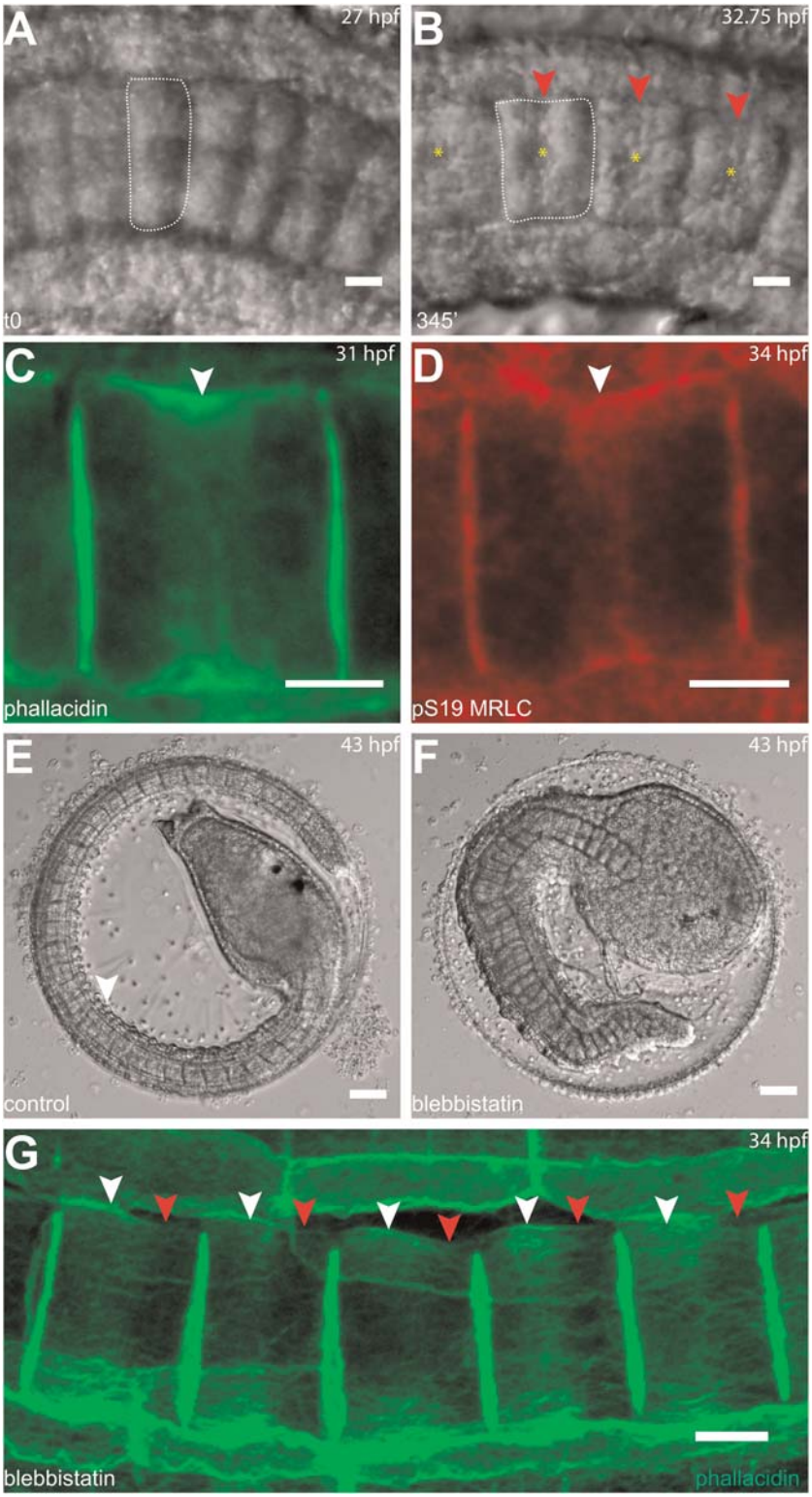

Figure 3. Circumferential actin rings are shifted anteriorly in *Halocynthia roretzi* notochord cells with centrally localized nuclei. (**A**, **B**) *Halocynthia* notochord cells elongate from coin-shaped (**A**) to drum-shaped (**B**). A circumferential constriction appears at the equator of the cylindrical cell (arrowhead). The nucleus (asterisk) is localized in the center of each cell. (**C**, **D**) Cortical F-actin (arrow in **C**) and MRLC (arrow in **D**) accumulate at the

Figure 3. continued on next page

Figure 3. Continued

equatorial region of the basal domain. (**E**, **F**) Notochord elongation (**E**, DMSO-treated) is abolished in *Halocynthia* embryos treated with 100 μM blebbistatin for 16 hr (**F**) starting at the onset of cell elongation (27 hpf). (**G**) Circumferential actin rings (white arrowheads) are shifted anteriorly after 3-hr blebbistatin treatment at 31 hpf (13˚C). Similar to what is observed in *Ciona* notochord cells (***Figure 2C′, H***), the shifted ring is associated with a circumferential bulge (white arrowheads), whereas the constriction is located posterior to the ring (red arrowheads). These results indicate (1) a conservation of the equatorial actomyosin contractile mechanism to drive notochord cell elongation in *Halocynthia*, (2) that the position of the ring does not influence the position of the nucleus, (3) the position of the nucleus does not influence the position of the ring, and (4) the nucleus position does not affect the direction of the ring shift. Anterior to the left in panels **A**–**B**, **G**. Scale bars in **E** and **F**, 50 μm; in all others, 10 μm.
DOI: 10.7554/eLife.09206.013

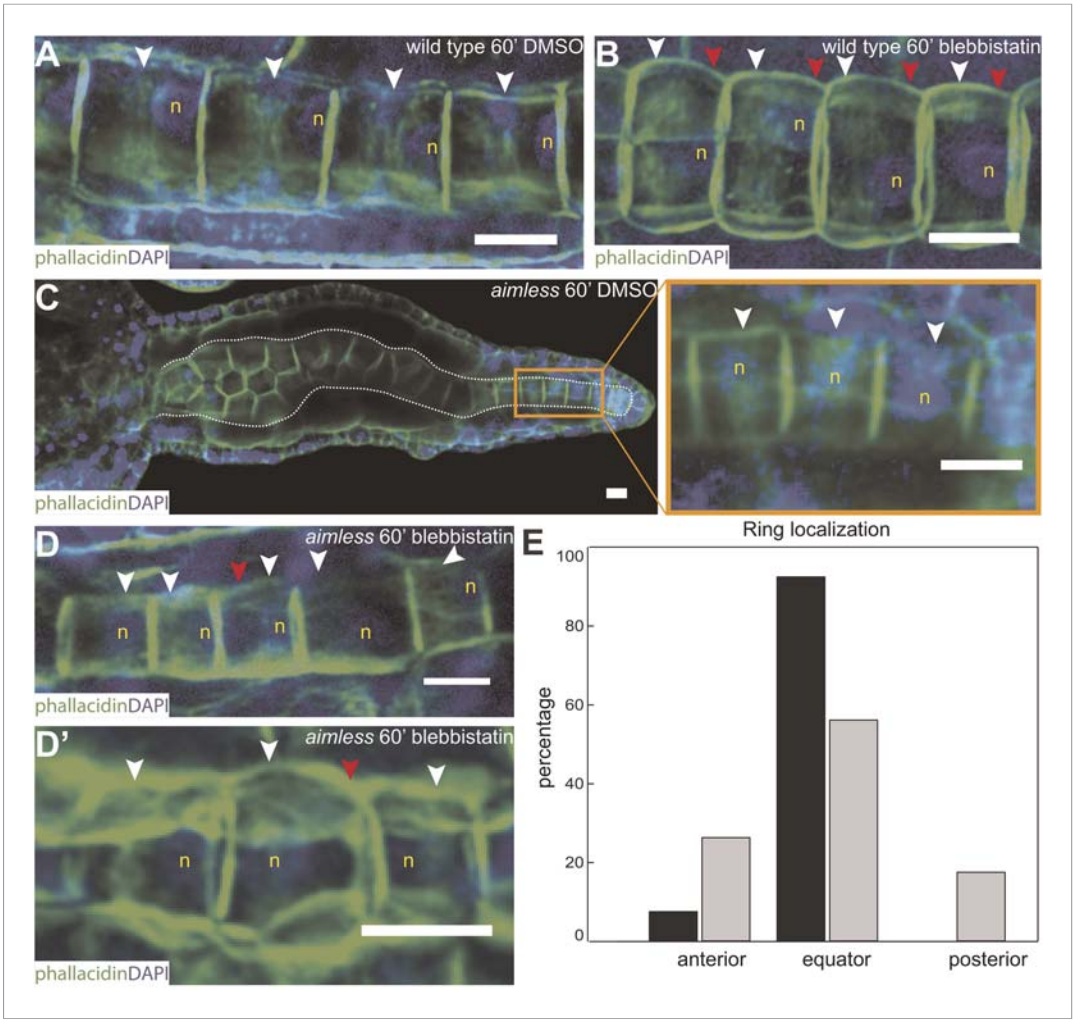

Figure 4. Anterior shifting of the actin ring is disrupted in the *prickle* mutant *aimless*. (**A**–**D'**) *Ciona savignyi* embryos are stained with phallacidin for actin and DAPI for nuclei. The actin ring (white arrowheads) is positioned at the equator in control notochord cells (**A**) and is shifted anteriorly by 60 min blebbistatin treatment (**B**), whereas the posterior localization of nucleus (n) is not affected by blebbistatin. Red arrowhead indicates the constriction. (**C**) Notochord in an *aimless* embryo (outlined by dashed line) with impaired cell intercalation in the anterior region, and fully intercalated and significantly elongated cells in the posterior region. The actin ring in these cells is localized at the equator, but the nucleus is placed in a random position (insert). (**D**, **D'**) 60-min blebbistatin treatment mislocalizes the actin ring in *aimless* embryos. (**E**) Distribution of actin rings in mock-treated (black; $n = 53$) and blebbistatin-treated (gray; $n = 57$) *aimless* cells. Anterior to the left in all panels. Scale bars, 10 μm.

DOI: 10.7554/eLife.09206.014

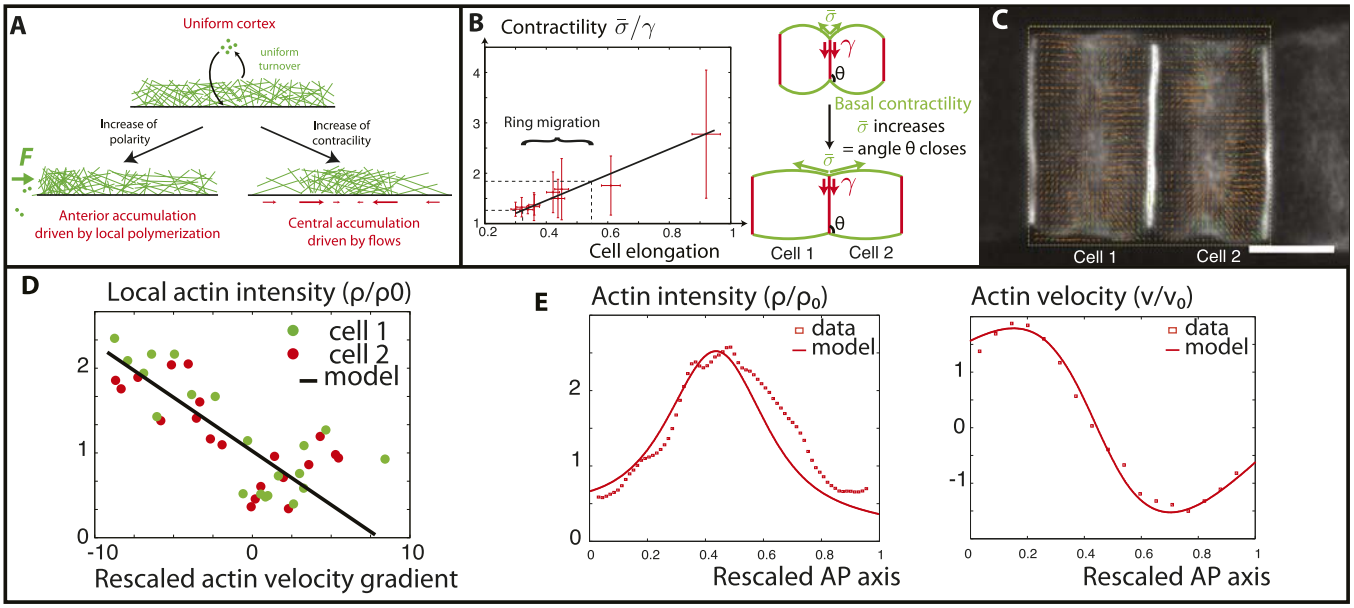

Figure 5. Verifications of the model assumptions and fitting of parameters. (**A**) Sketch of our model. Contractility destabilizes an initially homogenous cortex into a central ring, whereas PCP-driven preferential anterior polymerization localizes the ring on the edge. (**B**) Measurement of the angle between lateral and basal membrane during the elongation (2.5 increase) and ring migration (1.5 increase) process, which indicates their relative tensions (n > 15 for each time point). Basal tension increases with time. $\bar{\sigma}$ is the basal contractility, γ is the lateral contractility and θ is the angle between lateral and basal membranes. We have the geometric relation $\bar{\sigma}\cos\theta = \gamma$. (**C**) PIV analysis of cortical flows in late stage embryos. (**D**) Linear negative correlation between local actin intensity and velocity gradients, as extracted from PIV. Actin intensity and velocities have been rescaled in the dimensionless units described in the main text and in Appendix 2: rescaling. (**E**) Comparison between intensity and velocity profiles and our theoretical predictions (data extracted from **C**). The velocity field is rescaled by the average velocity.

DOI: 10.7554/eLife.09206.015

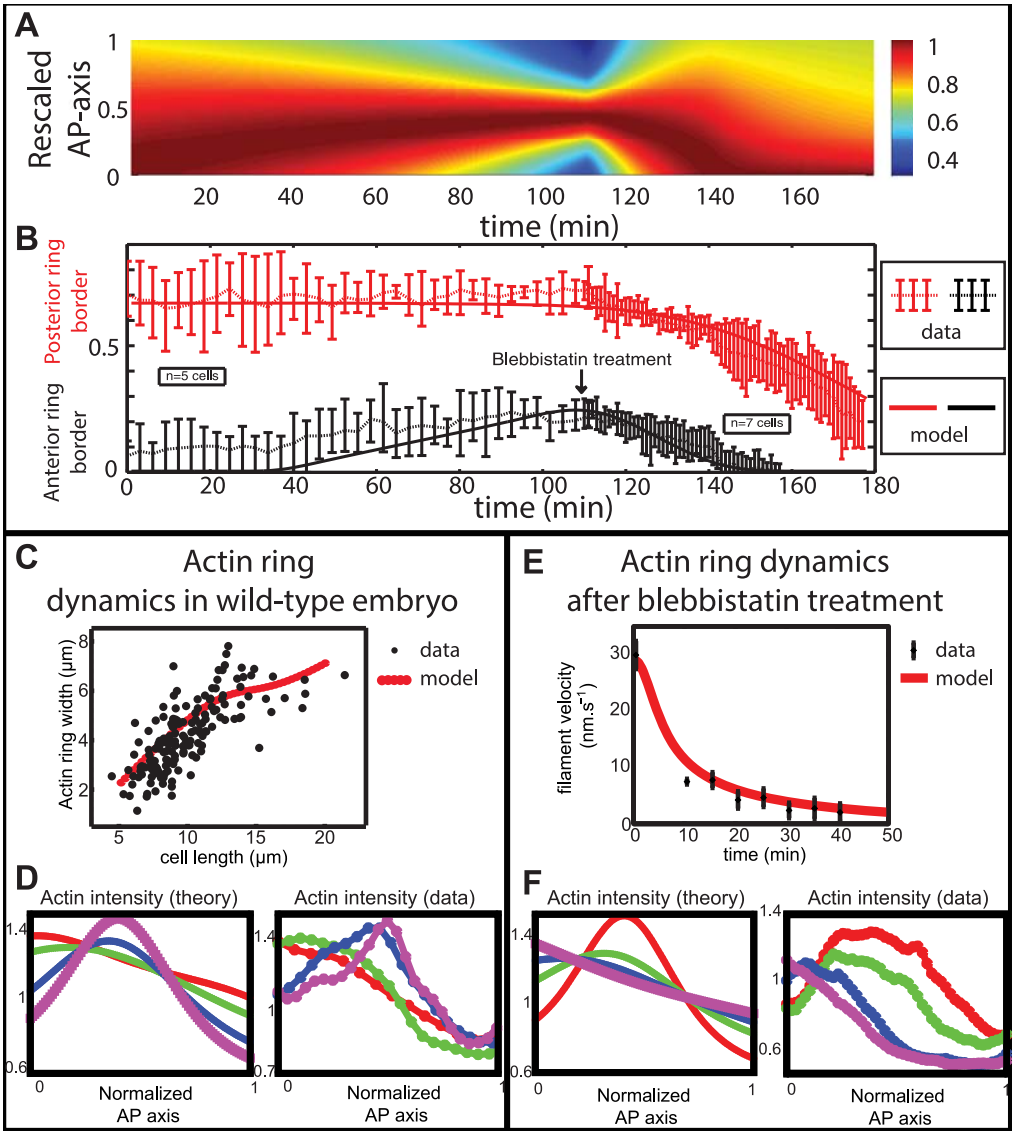

Figure 6. Comparison between theory and experiments on the dynamics of actin rings during migration and blebbistatin treatment. All theoretical curves are extracted from the same parameter set (see Appendix 5: model predictions for details on non dimensional values and parameters). (**A**) Kymograph of actin intensity during central ring migration (left part) and during blebbistatin treatment starting at 110 min. The color code indicates local actin intensity. (**B**) Comparison of the model and experimental anterior and posterior lateral domains during normal development (data taken from the average of 5 cells) and blebbistatin treatment at 110 min (data taken from the average of 7 cells). The y-axis indicates the position of the anterior and posterior border (defined as 50% of the ring maximal intensity). (**C**) Actin ring width vs with cell length, throughout cell elongation. The thick line is our theoretical prediction. The black dots are the measured data ($n = 7$; error bars = SEM). (**D**) Theory-to-experiment comparison of actin intensity profiles during central ring migration: 0 min (red), 30 min (green), 60 min (blue), 80 min (purple). (**E**) Theory-to-experiment comparison of filament velocity following blebbistatin treatment. (**F**) Theory-to-experiment comparison of actin intensity profiles after blebbistatin treatment: 0 min (red), 15 min (green), 30 min (blue), 45 min (purple).

DOI: 10.7554/eLife.09206.010

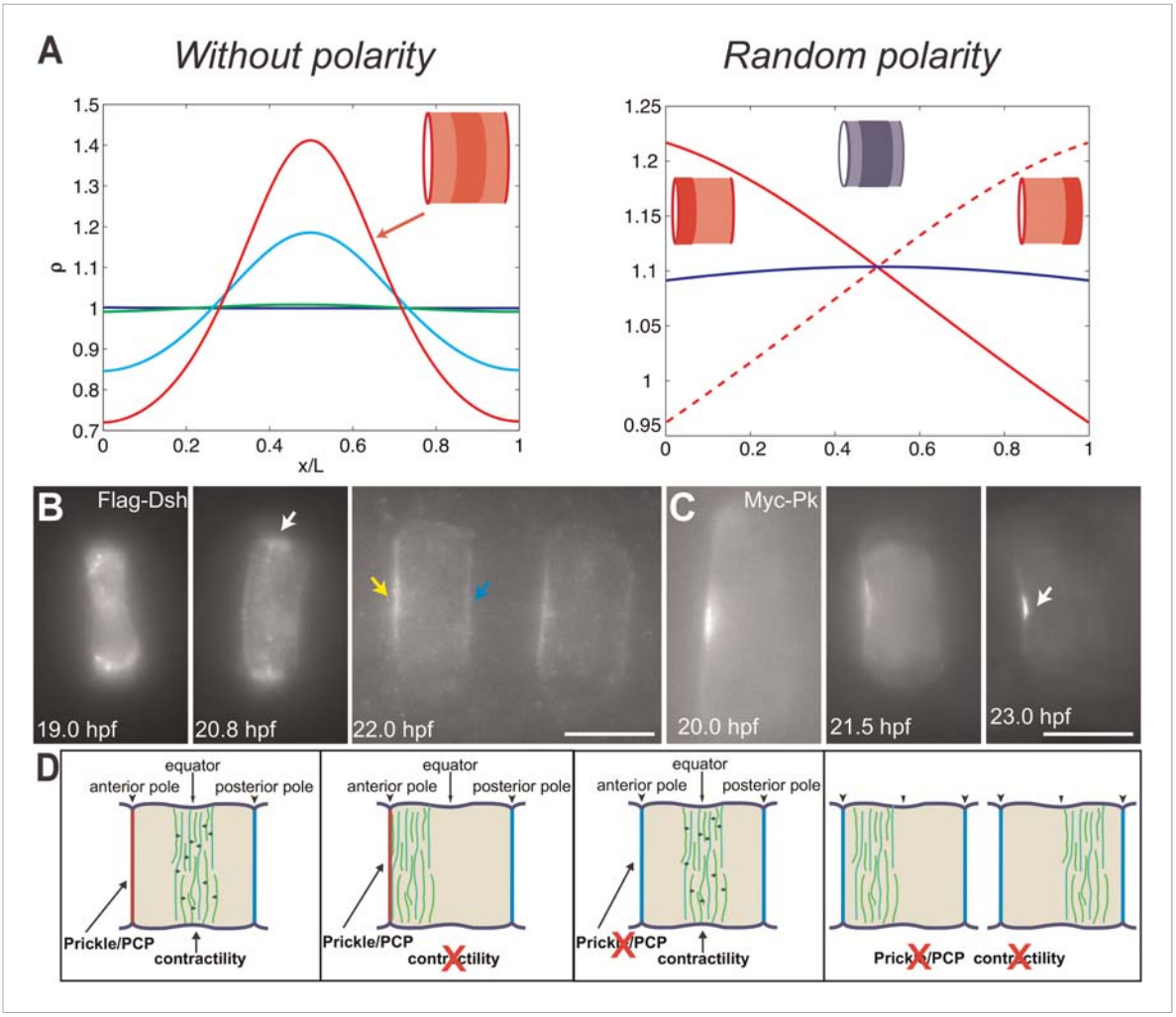

Figure 7. PCP participates in force balance to reposition actin rings. (**A**) Left: effect of a slow, 1.5-fold linear increase in contractility, for polarity-deficient mutants (no preferential flux on the edges). The ring forms directly at the center. Right: ring positioning for random uncoordinated polarity (preferential flux on the anterior, full red line, preferential flux on the posterior, dashed red line, and equal flux on anterior and posterior, full blue line). (**B**, **C**) Localization of Flag-Dsh (**B**), and Myc-Pk (**C**) in notochord cells. At early stages (19 and 20.8 hpf), Flag-Dsh localizes at the basal surface. At 20.8 hpf, it concentrates at the equator (white arrow). Subsequently, it shifts to both lateral surfaces, with a preference for anterior side of cells (yellow and blue arrows in **B**). Myc-Pk localizes at the anterior lateral surface of the cell at early stages and gradually concentrates to the center of anterior lateral surface (white arrow in **C**). (**D**) Myosin contractility antagonizes PCP to position a dynamic actin cytoskeleton. Anterior to the left. Scale bars, 10 μm.

DOI: 10.7554/eLife.09206.016